Proceedings of the 12th International IEEE Conference on Intelligent Transportation Systems, St. Louis, MO, USA, October 3-7, 2009

A Novel Approach for the Online Initial Calibration of Extrinsic Parameters for a Car-Mounted Camera

Stephanie Hold, Steffen Görmer, Anton Kummert
Faculty of Electrical, Information and Media Engineering
University of Wuppertal
D-42119 Wuppertal, Germany
{s.hold, goermer, kummert}@uni-wuppertal.de

Mirko Meuter, Stefan Müller-Schneiders
Delphi Electronics & Safety
D-42119 Wuppertal, Germany
{mirko.meuter,
Stefan.Mueller-Schneiders}@delphi.com

***Abstract*— This paper presents a novel approach for an online initial camera calibration to estimate the extrinsic parameters for vision-based intelligent driver assistance systems. The method uses the periodicity of dashed lane markings and velocity information to determine the extrinsic camera parameters: height, pitch and roll angle. A lane marking detector is utilized to convert the images of road scenes into a set of one-dimensional time series. Thereby, the lane marking detector samples the markings at predefined vertical coordinates in the image, so-called scanlines. Based on a correlation analysis and velocity information, the spatial shift between the scanlines is determined. Thus, the distances along the longitudinal lane markings are measured in the coordinate system of the vehicle independently of camera mounting parameters. The Gauss-Newton algorithm is implemented to minimize the squared error between these estimated distances and the distances obtained by the backprojection to a ground plane using the parameter dependent pinhole camera model. Finally, the approach is evaluated using synthetic and real data with promising results.**

I. Introduction

For active and passive safety, many sensors are installed to observe the traffic environment around the host vehicle. A vision sensor is commonly used to detect vehicles, traffic signs, lane markings or vulnerable road users in front of the vehicle. To be able to measure the real world distance of the vehicle to detected objects, the pose of the camera relative to the coordinate system of the vehicle has to be determined. Conventionally, the camera parameters are estimated based on controlled offline scenes, where 3D coordinates of a calibration pattern in the coordinate system of the vehicle are known. With respect to the production process or nomadic devices systems, the demand for convenient alternatives increases. Additionally, the system should be able to detect a decalibration and adjust the extrinsic parameters if required.

II. Previous Work

Conventionally, the camera pose is estimated by minimizing a nonlinear error function [1]. Exact 3D positions of fiducial markers in the target coordinate system are measured. After detecting the markers in the acquired images, a backprojection model is fitted by finding the describing parameters such as the three rotation angles and translational offsets. The main differences in offline calibration methods can be found in the choice of the fiducial markers, measurement technique, orientation of the calibration plane and the optimization algorithm [2], [3], [4], [5]. Additionally, many closed-form solutions have been proposed by several simplifications and linearization of the camera model [6], [7], [8]. Moreover, online calibration methods become more and more important in the automotive domain to ease the mounting step in the production process. Unlike in the case of offline approaches, 3D points in the coordinate system of the vehicle are not available. The basic idea is to use a priori information about traffic scenes. A common method is to use the road as calibration structure. Therefore, many assumptions about the traffic scenes are employed: e.g. parallelism of the lane markings, known road width, flat road, known movement of the vehicle, straight lane markings, equal length and spacing between longitudinal discontinuous stripes [9], [10], [11], [12], [13]. A well-known and simple approach to estimate the yaw and pitch angle is based on the detection of the horizon point. In [9], Southall and Taylor integrate additionally the estimation of the camera height based on a known lane width. Guiducci et al. [14] analyze the road width, length and spacing between longitudinal lane markings. In [10], image features are implemented to extract lane markings, zebra crossings and traffic signs. Zhaoxue and Pengfei [11] propose a method to calibrate the orientation, position and focal length. They analyze vanishing lines with identical known distances. Wu and An [12] present an extrinsic calibration method based on a parametrically described lane marking in the vehicle coordinate system using an Extended Kalman Filter. In [13], the extrinsic parameters are estimated by analyzing multiple consecutive frames moving straightforward with known displacements in the world. Extracting the road boundaries and objects with vertical edges, the rotation angles are computed by assuming a known height of the camera. In this paper, we propose a novel approach for an online initial estimation of the extrinsic parameters. A new method for the extraction of geometrical information is presented based on the periodic structure of dashed lane markings. The presence of dashed lane markings is verified by a lane type classification. Finally, the algorithm simultaneously approximates three of the camera mounting parameters: the height, pitch and roll angle.

978-1-4244-5521-8/09/$26.00 ©2009 IEEE

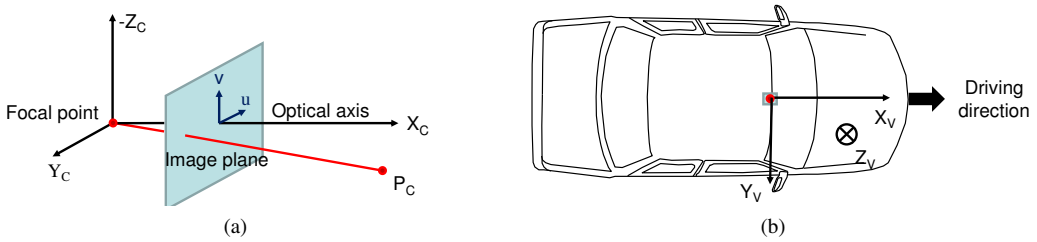

Fig. 1: Coordinate systems used: (a) coordinate system C-COS of the camera according to the pinhole camera model, (b) coordinate system V-COS according to the SAE conventions

III. Proposed Method

A. Overview

The presented approach estimates the extrinsic parameters by explaining extracted geometrical information of the world adapting the parameters of a camera model. Assuming the presence of dashed lane markings, lane markings are detected at predefined vertical coordinates in the image, so-called scanlines. The detection results, lane markings detected or not detected, are saved into a one-dimensional time-series for each scanline. The extraction of geometrical information is done by analyzing the correlation between the set of time series. Finally, the extrinsic parameters are estimated by a nonlinear optimization algorithm.

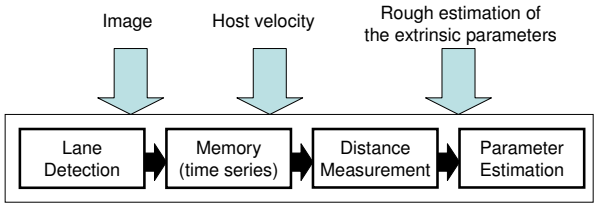

Fig. 2: Overview of the calibration method

B. Problem Formulation

A monocular camera mounted behind the windscreen of the vehicle looks forward and observes the traffic environment. To localize observed objects, it is essential to know the spatial relationship between the coordinate system of the camera and the vehicle. Therefore, two conventional coordinate systems are used.

1) Coordinate system of the camera: Fig. 1a shows the coordinate system of the camera (C-COS), defined accordingly to the simple pinhole model with the three axes x_C, y_C and z_C. The only difference to the simple pinhole model is the orientation of the axes to simplify the formulation of the rotation matrix. The origin lies in the focal point and the image plane perpendicular to the x_c- axis, the principle axis, in a distance of f, the focal length. u, v are coordinates in the image plane.

2) Coordinate system of the vehicle: The coordinate system of the vehicle (V-COS) is visualized in fig. 1b. The origin of the V-COS is fixed to the intersection point of the perpendicular line of the focal point of the camera and the ground plane. The orientation of the three axes x_V, y_V and z_V accords to the SAE convention. x_V is directed in driving direction.

We are interested in the projection of the image plane onto the ground plane, which means a 2D/2D mapping. The spatial relationship of the two coordinate systems C-COS and V-COS describes the mounting of the camera. It is specified by a translation vector $\mathbf{t}$ for the height h of the camera and a rotation matrix $\mathbf{R}$ for the three angles (fig. 3). The rotation matrix $\mathbf{R}$ is described as the multiplication of the individual rotation matrices about the single axes. The rotation about the Y_V-axis is denoted as tilt angle α, about the X_V-axis as roll angle β and about the Z_V-axis as pan angle γ. The translation vector $\mathbf{t}$ and the rotation matrix $\mathbf{R}$ acclaim with $c_\alpha = \cos\alpha$, $s_\alpha = \sin\alpha$, $c_\beta = \cos\beta$, $s_\beta = \sin\beta$, $c_\gamma = \cos\gamma$ and $s_\gamma = \sin\gamma$:

$$\mathbf{t} = \begin{pmatrix} 0 & 0 & -h \end{pmatrix}^T \tag{1}$$

$$\mathbf{R} = \begin{pmatrix} c_\alpha c_\beta & -c_\alpha s_\gamma & -s_\alpha \\ -s_\alpha s_\beta c_\gamma + s_\gamma c_\beta & s_\alpha s_\beta s_\gamma + c_\beta c_\gamma & -c_\alpha s_\beta \\ c_\alpha c_\beta c_\gamma + s_\beta s_\gamma & -s_\alpha c_\beta s_\gamma + s_\beta c_\gamma & c_\alpha c_\beta \end{pmatrix} \tag{2}$$

Thus, every point $\mathbf{p}_C = \begin{pmatrix} X_C & Y_C & Z_C \end{pmatrix}^T$ in the C-COS

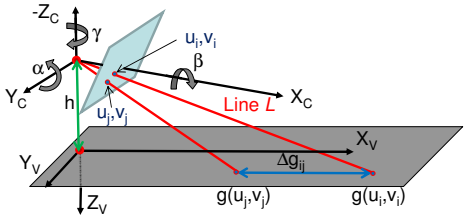

Fig. 3: Projection model of the image plane onto the ground plane

can be transformed into a point $\mathbf{p}_V = \begin{pmatrix} X_V & Y_V & Z_V \end{pmatrix}^T$ in the V-COS.

$$\mathbf{p}_V = \mathbf{R} \cdot \mathbf{p}_C + \mathbf{t} \tag{3}$$

Every point $\mathbf{p}_C$ on the image plane can be calculated by backprojection. Therefore, a unit vector is defined as the normalized connection vector $\mathbf{m}_V$ between the image point $\mathbf{p}_C = \begin{pmatrix} -f & u & v \end{pmatrix}^T$ and the focal point. Every point $\mathbf{p}_V$ on the backprojection line L defined through the normalized

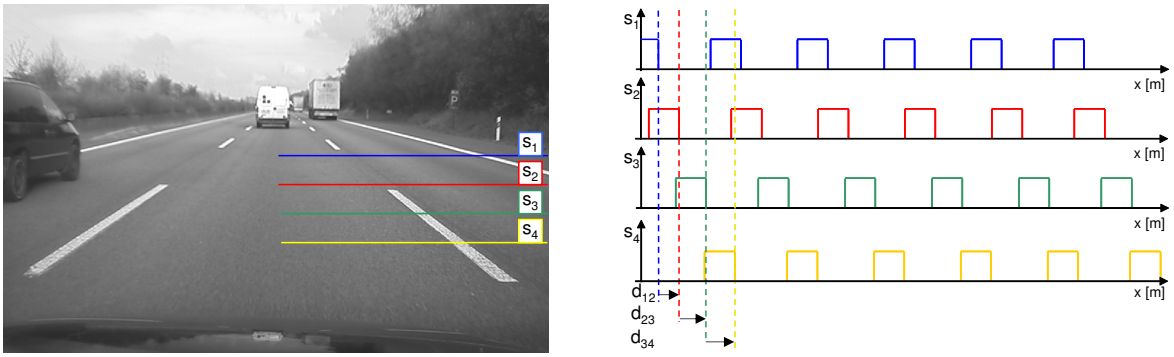

(a) (b)

Fig. 4: (a) Sampling approach based on scanlines, (b) signals with different spatial phases

connection vector $\mathbf{m}_V$ and a position vector $\mathbf{t}$ are written as:

$$\mathbf{p}_V = \mathbf{t} + \lambda \mathbf{m}_V \tag{4}$$

The ground plane of the road is described by the well-known plane function defined by the unit vector $\mathbf{n}_V = \begin{pmatrix} 0 & 0 & 1 \end{pmatrix}^T$:

$$\mathbf{p}_V \cdot \mathbf{n}_V = 0 \tag{5}$$

Thus, the intersection point of the line L and the ground plane can be calculated. The X_V-coordinate of the V-COS results

$$g(u,v) = \frac{h \cdot (f \cdot \mathrm{c}\alpha + u \cdot \mathrm{c}\alpha\mathrm{s}\beta + v \cdot \mathrm{s}\alpha)}{f \cdot \mathrm{s}\alpha\mathrm{c}\beta + u \cdot \mathrm{s}\alpha\mathrm{c}\beta\mathrm{s}\gamma - u \cdot \mathrm{s}\beta\mathrm{c}\gamma - v \cdot \mathrm{c}\alpha\mathrm{c}\beta} \tag{6}$$

The intrinsic parameters, namely the focal length f, the principle point and the pixel size are calibrated by the method proposed in [15]. To estimate the so-called extrinsic parameters $\mathbf{p} = \begin{pmatrix} h & \alpha & \beta \end{pmatrix}^T$, describing the spatial relationship of the C-COS and V-COS, corresponding information has to be extracted. As introduced in section II, a very common method is to define a set of points and measure the 3D-coordinates in both coordinate systems. For a driving vehicle in an unknown environment, the conventional point-based method is not possible. Our approach uses relative information, measured distances d_{ij} between points $\mathbf{p}_{C,i}$ and $\mathbf{p}_{C,j}$ along the x_V-axis in driving direction, instead of their absolute coordinates [16].

Therefore, a measurement function Δg is defined as the Euclidean distance between two points $\mathbf{p}_{C,i}$ and $\mathbf{p}_{C,j}$ in the V-COS.

$$\Delta g(\mathbf{p}; u_i, v_i, u_j, v_j) = g(\mathbf{p}; u_i, v_i) - g(\mathbf{p}; u_j, v_j) \tag{7}$$

An error function $\varepsilon(\mathbf{p}; u_i, v_i, u_j, v_j)$ is defined depending on the extrinsic parameters $\mathbf{p}$.

$$\varepsilon(\mathbf{p}; u_i, v_i, u_j, v_j) = \Delta g(\mathbf{p}; u_i, v_i, u_j, v_j) - d_{ij} \tag{8}$$

C. Lane Detection and Memory

Based on a conventional lane detector, the lane markings can be sampled in each frame at predefined v_i-coordinates, so-called scanlines (fig. 4a). The scanlines are defined depending on the intrinsic parameters and a rough estimation of the extrinsic parameters. The results of the lane detector are saved into a set of time series $s_i(k)$ which are called signals, where i describes the number of the corresponding scanline. These signals are defined for K frames with $k \in \{1, \ldots, K\}$ as:

$$s_i(x) = \begin{cases} 1 & \text{if lane marking is present} \\ 0 & \text{otherwise} \end{cases} \tag{9}$$

The resulting signals of dashed lane markings are described as sampled periodic rectangle functions. They are distinguishable by their different spatial phases (fig. 4b). The frame number k corresponds to the driven distance x, which is calculated by the inertial sensors of the vehicle. Because of varying velocities, the spatial sampling rate is not constant. The signals are resampled using a linear interpolation to obtain an equidistant spatial sampling period. The frame rate is assumed to be known.

D. Distance Measurement

A similar problem to the estimation of spatial phases between the signals can be found in various other applications, e.g. in medical imaging, radar and acoustics signal processing. Many solutions are presented in literature for the so-called time delay estimation problem between signals acquired by different sensors and replicas of signals [17]. A commonly discussed issue is how to achieve subsample accuracy in an adequate processing time.

Basically, there are two common approaches for the estimation of the spatial phase. The first is based on the analysis of the cross correlation coefficient function [18]. The spatial phase can be extracted through peak detection or locating the zero-crossing of its Hilbert transform [19]. Secondly, the spatial phase can be determined through the slope of the cross spectral phase [20].

The estimation of the spatial shift based on the cross correlation function demands a lot of computation time. Those approaches require expensive interpolation and resampling methods. Furthermore, the estimation accuracy is biased. Estimation methods based on the analysis in the frequency domain are much faster because of the Fast Fourier Transform. In the following, the method and its basic idea are described.

For the spectral analysis, the Fourier Transform $S_i(k_x)$ of the signal $s_i(x)$ is calculated depending on the spatial

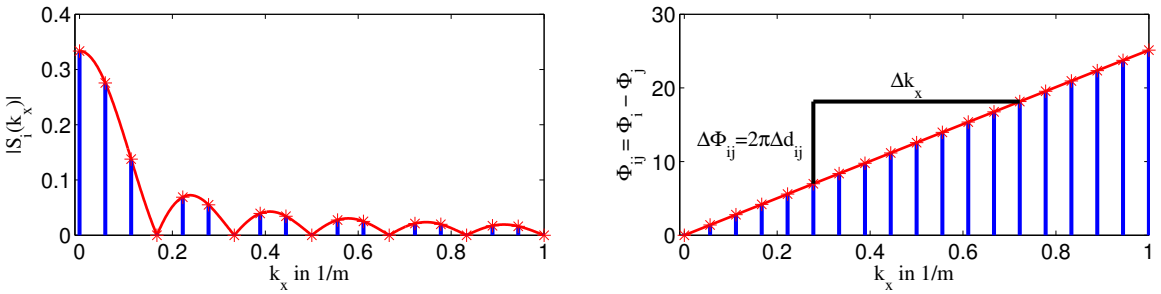

(a) (b)

Fig. 5: (a) Fourier Transform of an analogue lane marking signal (theoretic analysis) (b) Difference of the spatial phases between two different scanlines i and j

frequency k_x.

$$S_i(k_x) = \int s_i(x)\, e^{-2\pi j k_x x} dx \tag{10}$$

The signal $s_i(x)$ of a dashed lane marking is described by a periodic rectangle function, which can be expressed as the convolution of a single rectangle with the width l with a dirac comb. L represents the period length. The Fourier Transform is a modified si-function (fig. 5a).

$$s_i(x) = \frac{1}{l}\text{rect}\left(\frac{x}{l}\right) * \sum_{n=-\infty}^{\infty} \delta(x - nL) \tag{11}$$

$$S_i(k_x) = \frac{l}{L}\text{si}(\pi l k_x) \cdot \sum_{n=-\infty}^{\infty} \delta\left(k_x - \frac{n}{L}\right) \tag{12}$$

The Fourier Transform is approximated by a Discrete Fourier Transform. Assuming dashed lane markings on German highway, the spectral leakage is negligible for velocities up to 200 km/h by choosing a suitable window function, a Hamming window. The choice of the length of the temporal window assures a sufficient spectral resolution.

The difference between the sampled signals of two different scanlines i and j is a spatial displacement d_{ij}.

$$s_j(x) = s_i(x - d_{ij}) \tag{13}$$

Based on a property of the Fourier transform, the spatial displacement is correlated with a phase shift in the frequency domain. The phase shift is linear and proportional to the amount of the spatial displacement and the frequency.

$$s_j(x) = s_i(x - d_{ij}) \circ\!\!-\!\!\bullet S_i(k_x)\, e^{-i2\pi k_x d_{ij}} \tag{14}$$

The signals $s_i(x)$ and $s_j(x)$ of the scanlines i and j differ in their phase. The difference of their phases Φ_{ij} is linear with the slope $\Delta\Phi_{ij}$ (fig. 5b).

$$\Phi_{ij} = \Phi_i(k_x) - \Phi_j(k_x) \tag{15}$$

$$\Delta\Phi_{ij} = 2\pi d_{ij} \tag{16}$$

Thus, the spatial displacement d_{ij} is estimated by approximating the difference of the phases Φ_{ij}.

$$d_{ij} = \frac{\Delta\Phi_{ij}}{2\pi} \tag{17}$$

E. Parameter Estimation

The estimation of the camera pose can be described as a nonlinear least square problem (fig. 6). The optimization task is to minimize the error between measured distances d_{ij} in the world and distances $\Delta g(\mathbf{p}; u_i, v_i, u_j, v_j)$ obtained by backprojection based on a camera model varying the extrinsic parameters $\mathbf{p}$.

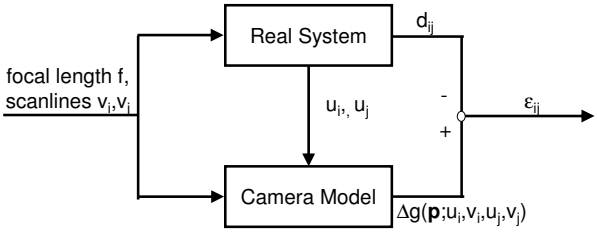

Fig. 6: Optimization strategy

The error function is:

$$\varepsilon(\mathbf{p}) = \begin{pmatrix} \varepsilon(\mathbf{p}; u_1, v_1, u_2, v_2) \\ \varepsilon(\mathbf{p}; u_2, v_2, u_3, v_3) \\ \vdots \\ \varepsilon(\mathbf{p}; u_{n-1}, v_{n-1}, u_n, v_n) \end{pmatrix} \tag{18}$$

The Gauss-Newton strategy [21] is used to solve the non-linear equalization problem based on the method of least squares.

$$\mathbf{p}^* = \arg\min_{\mathrm{p}} \|\varepsilon(\mathbf{p})\|^2 \tag{19}$$

Note that $\varepsilon(\mathbf{p})$ is differentiable and an initial estimate $\mathbf{p}_0$ is available. Based on a Taylor Expansion around the current estimate for $\mathbf{p}_k$, a linear equation problem is solved for every iteration step k.

$$\nabla\varepsilon(\mathbf{p}_k)^T \nabla\varepsilon(\mathbf{p}_k)\, d\mathbf{p}_k = \nabla\varepsilon(\mathbf{p}_k)^T \varepsilon(\mathbf{p}_k) \tag{20}$$

Based on the symmetry of the positive-definite matrix $\nabla\varepsilon(\mathbf{p}_k)^T \nabla\varepsilon(\mathbf{p}_k)$, its inversion is done by the Cholesky factorization.

$$d\mathbf{p}_k = \left[\nabla\varepsilon(\mathbf{p}_k)^T \nabla\varepsilon(\mathbf{p}_k)\right]^{-1} \nabla\varepsilon(\mathbf{p}_k)^T \tag{21}$$

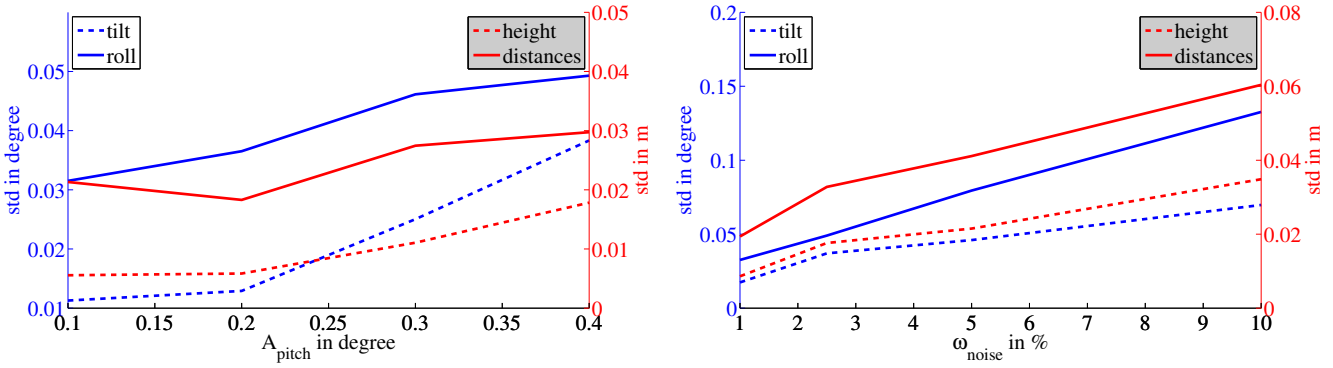

(a) (b)

Fig. 7: Results achieved in the simulation: (a) shows the uncertainties of the height, distances, the tilt and roll angles dependent on the noise level, (b) shows the uncertainties of the height, distances, the tilt and roll angles dependent on the pitching amplitude

The next estimate for the parameter results in

$$\mathbf{p}_{k+1} = \mathbf{p}_k + d\mathbf{p}_k \tag{22}$$

IV. Results

The evaluation of the presented calibration method is divided into a theoretical analysis based on synthetic data and a test on reproducibility based on real data. Within the evaluation, eight measurements calculated on time series with 500 frames for each side are taken into account.

Image Size [Pixel]	Pixel Pitch [µm]	Focal Length [mm]	Principle Point [Pixel]
750 × 480	6	6.035	(399, 238)

TABLE I: Intrinsic parameters of the simulated and real camera

Height [m]	Tilt [degree]	Roll [degree]	Pan [degree]
1.3	-5.7	-0.5	0

TABLE II: Extrinsic parameters of the simulated camera

A. Simulation

A straight and flat road is defined in a fixed vehicle coordinate system. The borders of the road with a width of 3.5 m are marked by dashed lane markers. Now, a car is driving along this virtual road with a velocity of 100 km/h and acquiring virtual images based on a simple pinhole model characterized by the camera parameters of table I and table II. Five scanlines are defined. The whole length of the virtual road accounts 20 km. The frame rate is assumed to be constant at 30 Hz. The calculation of standard deviation is based on randomly selected 25 samples. In the following, the influence of several error sources are examined.

a) Discretization: In a first step, the effects of the discretization are analyzed. The resulting standard deviation of the true data accounts for the extrinsic parameter: 0.01 degree for the tilt angle, 0.03 for the roll angle and 5 mm for the height.

b) Errors in Lane Detection: Errors of the lane detection are modeled by binary noise. Different noise levels ω_{noise} are defined, which represent the relation between false and true samples in the sets of time series. Figure 7b shows the averaged absolute difference between the true and estimated camera parameters.

c) Pitching: In this paper, pitching caused by road irregularities is modeled as superposed sine-functions with attenuated amplitudes. The amplitude A_{pitch} is a normal distributed variable $\mathcal{N}(0, A_{\text{pitch}})$. The attenuation is characterized by $a = 2/s$ and the frequency by $f = 1/s$. At every discrete point in time t_n, the system is initiated to oscillate. t_n is uniformly distributed. The number of samples depends on the road roughness. The pitching angle is:

$$\Delta\alpha = \sum_{n=1}^{N} A_{\text{pitch}} e^{-a(t-t_n)} \sin\left[2\pi f \cdot (t-t_n)\right] \cdot u\left(t_n\right) \tag{23}$$

Analogous to the visualization of the previous results, figure 7a shows the dependence of the mean amplitude and the uncertainty of the estimation.

d) Driving not exact parallel: Based on the output of lane departure warning systems, a varying lateral distance y_V to the lane markings is assumed. The distance varies approximately according to a sine-function with a periodic length of about $1/f = 800\text{m}$. The amplitude A_{lat} is the variable.

$$y_V = A_{\text{lat}} \cdot \sin\left(2\pi f \cdot t\right) \tag{24}$$

Caused by the varying distances to the lane markings, the driving direction of the vehicle is not exactly parallel to the lane. Based on the described varying distance, the maximum constant angle accounts approximately 0.13 degree. This has a negligible influence on the u-position in the image and on

the measured distances. The angle can be interpreted as a yaw angle which does not have any significant influence on the distances. The movement in driving direction is estimated too big, because the velocity information of the car has to be divided into a longitudinal and lateral part. Thus, also the periodic length and the distances exhibit a systematic offset.

e) Inexact velocity and looptime measurement: Inexact velocity and looptime measurement affects the sample date. It has to be differentiated between systematic and random errors. Systematic errors caused by legal specifications or differing tire diameters can be eliminated by normalization with the ratio of the expected and detected frequency of the lane markers. The influence of noisy time measurments is analyzed by simulating normal distributed additive noise dx.

$$x = \bar{x} + dx \tag{25}$$

The results show that the realistic noise has no significant influence on the estimation accuracy.

B. Real Data

Image sequences showing more than 10 km of German highways are acquired in over 12000 frames. The intrinsic parameters of the camera are summarized in table I. The mean velocity is approximately 100 km/h. The marklets at the predefined scanlines are manually annotated in these sequences. To analyze the reproducibility of the proposed calibration method, the sequences are divided into several subsets with 500 frames each. The reproducibility is represented in the standard deviation of the extrinsic parameters visualized in table III. With uncertainties less than 0.04 degree for the pitch angle, 1.5 cm for the camera height and 0.07 degree for the roll angle, the results are very promising. Experiments with the system utilizing a lane detection algorithm [22] showed good results in accordance to the previously presented evaluation.

Height [m]	Tilt [degree]	Roll [degree]
mean(h) +/- std (h)	mean(α) +/- std (α)	mean(β) +/- std (β)
1.30+/-0.014	-5.56+/-0.04	-0.52+/-0.07

TABLE III: Estimated extrinsic parameters of the real camera and its standard deviations

V. Conclusions

An online initial extrinsic calibration approach for a car-mounted camera has been presented. The algorithm exhibits the advantage that no exact known 3D measurements of points are required. Compared to conventional online approaches, the algorithm needs only distances in the world which can be measured independently of the length of longitudinal lane markers and spaces and the camera model parameter. Furthermore, due to the sampling approach based on lane detection at few predefined scanlines, a high performance detection algorithm can be chosen. The evaluation based on synthetic and real data shows very promising results.

Future work includes the development of a robust initial estimation of the extrinsic parameter and the choice of a suitable marklet detector.

References

[1] C. C. Slama. *Manual of Photogrammetry*. American Society for Photogrammetry, 1980.

[2] M. Bellino, Y. L. de Meneses, S. Kolski, and J. Jacot. Calibration of an embedded camera for driver-assistant systems. In *Proc. IEEE Intelligent Transportation Systems*, pages 354–359, 13–15 Sept. 2005.

[3] S. Ernst, C. Stiller, J. Goldbeck, and C. Roessig. Camera calibration for lane and obstacle detection. In *Proc. IEEE/IEEJ/JSAI International Conference on Intelligent Transportation Systems*, pages 356–361, 5–8 Oct. 1999.

[4] T. Marita, F. Oniga, S. Nedevschi, T. Graf, and R. Schmidt. Camera calibration method for far range stereovision sensors used in vehicles. In *Proc. IEEE Intelligent Vehicles Symposium*, pages 356–363, 2006.

[5] A. Bodis-Szomoru, T. Daboczi, and Z. Fazekas. A far-range off-line camera calibration method for stereo lane detection systems. In *Proc. IEEE Instrumentation and Measurement Technology*, pages 1–6, May 2007.

[6] R. Tsai. A versatile camera calibration technique for high-accuracy 3d machine vision metrology using off-the-shelf tv cameras and lenses. 3(4):323–344, August 1987.

[7] Y. I. Abdel-Aziz and H. M. Karara. Direct linear transformation into object space coordinates in close-range photogrametry. In *Proc. Symp. Close-Range Photogrametry*, pages 1–18, 1971.

[8] T. Melen. *Geometrical Modelling and Calibration of Video Cameras for Underwater Navigation*. PhD thesis, Norwegian Univ. of Science and Technology, Trondheim, Norway, 1994.

[9] B. Southall and C. J. Taylor. Stochastic road shape estimation. In *Proc. Eighth IEEE International Conference on Computer Vision*, volume 1, pages 205–212, 7–14 July 2001.

[10] U. Franke, D. Gavrila, S. Gorzig, F. Lindner, F. Puetzold, and C. Wöhler. Autonomous driving goes downtown. *IEEE Intelligent Systems and Their Applications*, 13(6):40–48, Nov.–Dec. 1998.

[11] C. Zhaoxue and S. Pengfei. Efficient method for camera calibration in traffic scenes. *Electronics Letters*, 40(6):368–369, 18 March 2004.

[12] Meng Wu and Xiangjing An. An automatic extrinsic parameter calibration method for camera-on-vehicle on structured road. In *Proc. Conference on Vehicular Electronics and Safety IEEE International*, pages 1–5, 13–15 Dec. 2007.

[13] H. J. Lee and C. T. Deng. Camera models determination using multiple frames. In *Proc. IEEE Computer Society Conference on Computer Vision and Pattern Recognition*, pages 127–132, 3–6 June 1991.

[14] A. Guiducci. Camera calibration for road applications. *Computer Vision and Image Understanding*, 79(2):250–266, 2000.

[15] J. Y. Bouguet. Camera calibration toolbox for matlab. www.vision.caltech.edu/bouguety.

[16] S. Hold, C. Nunn, S. Müller-Schneiders, and A. Kummert. Efficient and robust extrinsic camera calibration procedure for lane departure warning. In *Proc. IEEE Intelligent Vehicles Symposium*, pages 382–387, 2009.

[17] M. Matassoni and P. Svaizer. Efficient time delay estimation based on cross-power spectrum phase. In *Proc. 14th European Signal Processing Conference*, 2006.

[18] B. Qin, H. Zhang, Q. Fu, and Y. Yonghong. Subsample time delay estimation via improved gcc phat algorithm. In *Proc. International Conference on Signal Processing*, pages 2579–2582, 2008.

[19] R. Cabot. A note on the application of the hilbert transform to time delay estimation. *IEEE Transactions on Acoustics, Speech and Signal Processing*, 29(3):607–609, 1981.

[20] G. Nolte, A. Ziehe, V. V. Nikulin, A. Schlögl, N. Krämer, T. Brismar, and K.-R. Müller. Robustly estimating the flow direction of information in complex physical systems. *Physical Review Letters*, 100(23):234101, 2008.

[21] D. G. Lowe. Fitting parameterized three-dimensional models to images. 13(5):441–450, May 1991.

[22] R. Risack, P. Klausmann, W. Krüger, and W. Enkelmann. Robust lane recognition embedded in a real-time driver assistance system. In *Proc. IEEE Intelligent Vehicles Symposium*, pages 35–40, 1998.